Available online at www.sciencedirect.com
ScienceDirect
Thermochimica Acta 467 (2008) 117–120
thermochimica acta
www.elsevier.com/locate/tca

Short communication

Thermal behaviour of low and high molecular weight paraffin waxes used for designing phase change materials

A.S. Luyt [a,*], I. Krupa [b]

[a] Department of Chemistry, University of the Free State (Qwaqwa Campus), Private Bag X13, Phuthaditjhaba 9866, South Africa
[b] Polymer Institute, Slovak Academy of Sciences, Dúbravská cesta 9, 842 36 Bratislava, Slovakia

Received 27 July 2007; received in revised form 1 November 2007; accepted 1 November 2007

Abstract

Two waxes, a soft petroleum wax and a hard Fischer–Tropsch paraffin wax, have been investigated to find the reasons for multiple endothermic peaks observed during heating in a DSC. DSC curves, molar mass distribution curves, and variable-temperature XRD results were compared, and it was confirmed that the first endothermic peak for the soft petroleum wax was due to a solid–solid transition, while the second endothermic peak was due to melting. However, for the hard Fischer–Tropsch paraffin wax there was no evidence of a solid–solid transition, and it was concluded that the multiple endothermic peaks in this case were due to melting of different molar mass fractions.
© 2007 Elsevier B.V. All rights reserved.

Keywords: Wax; Multiple peaks; DSC; XRD

1. Introduction

Paraffin waxes are saturated hydrocarbon mixtures, normally consisting of a mixture of different alkanes. They are frequently used as phase change materials (PCMs) for thermal storage applications because of their desirable characteristics, such as high latent heat of fusion, negligible super-cooling, low vapor pressure in the melt, chemical inertness and stability. The carbon atom chain lengths for paraffin waxes with a melting temperature between 30 and 90 °C range from 18 to 50 (C18–C50). Increased length of the carbon atom chains increases molecular weight and results in a higher melting temperature of the material. The specific heat capacity of paraffin waxes is about 2.1 kJ kg^{-1} K^{-1}. Their melting enthalpy lies between 180 and 230 kJ kg^{-1}, which is very high for organic materials. The combination of these two values results in an excellent energy storage density [1]. This complex behaviour makes them ideal candidates for using as PCMs [2,3].

PCMs have received great interest in many applications such as energy storage and thermal protection systems, as well as in active and passive cooling of electronic devices [4–6]. Thermal energy storage is one of the most important applications of PCM. In this case, PCM enables the temporary storage of high or low temperature energy for later use. It bridges the time gap between energy requirements and energy use and contributes to the effective use of energy. Basically, the only phase change used for PCMs is the solid–liquid change. Different inorganic as well as organic substances were already employed for the creation of PCMs; paraffin waxes belong to the most prospective ones [7].

The high melting enthalpy of paraffin waxes is associated with the fact that paraffins have a high degree of crystallinity. The applicability of paraffin waxes for PCM applications is dominated by the crystallization properties resulting from the composition. It is known that various crystal polymorphic structures are formed by various alkanes. The stable low temperature phase is typically the triclinic or orthorhombic crystalline structure for short chain alkanes, although monoclinic and hexagonal structures have also been observed [8,9]. The crystalline structure is influenced by a unique mesophase observed in some alkanes. This mesophase, termed the plastic crystalline or rotator phase, occurs in a narrow temperature range, although several rotator phases may exist between the crystalline phase and the isotropic liquid state [10,11].

This feature of paraffin waxes was frequently observed and investigated, especially in the case of low molecular weight paraffin waxes. As we have shown recently [12–15], high

* Corresponding author.
E-mail address: luytas@qwa.uovs.ac.za (A.S. Luyt).

0040-6031/$ – see front matter © 2007 Elsevier B.V. All rights reserved.
doi:10.1016/j.tca.2007.11.001

molecular weight Fischer–Tropsch (FT) paraffin waxes have completely different behaviour than low molecular weight petroleum waxes. We showed that the DSC heating curve of pure Wax FT depicts two endothermic peaks which are positioned at about 72 and 95 °C (for different FT waxes it changes, but the trend is the same). We discussed that the first peak may relate to the solid–solid transition between two different crystalline phases, but the multiple peaks may also be the result of the melting of different crystalline phases. It was confirmed that the second peak is associated with the melting of crystallites. However, these peaks are not so unambiguously separated as in the case of low molecular weight petroleum waxes. They lie closer to each other and overlap.

In this paper we discuss the thermal transitions of a low molecular weight petroleum wax and a high molecular weight Fischer–Tropsch paraffin wax, both of which we have used in previous PCM research [15,16]. The main purpose of this communication is to explain the multiple peaks observed for the Fischer–Tropsch paraffin wax in comparison to the soft petroleum wax. The thermal behaviour of the soft petroleum wax is in line with that observed and discussed in a number of published papers [8–11,22–26].

2. Experimental

2.1. Materials

The following materials were investigated: hard, brittle, straight-hydrocarbon chain paraffin wax (average molar mass = 785 g mol^{-1}, density = 0.940 kg L^{-1}) (Sasol Wax, Sasolburg, South Africa)—Wax FT; soft paraffin wax (carbon number C18–C40, average molar mass = 374 g mol^{-1}, density = 0.919 kg L^{-1}) (Slovnaft, Slovakia)—Wax S.

2.2. Differential scanning calorimetry (DSC)

Differential scanning calorimetry was carried out in a PerkinElmer DSC7 differential scanning calorimeter under nitrogen flow (20 mL min^{-1}). Samples (5–10 mg weighed to 0.1 mg precision) were heated from −20 to 100 °C (Wax S) and from 25 to 150 °C (Wax FT) at a heating rate of 10 °C min^{-1} and then cooled at the same rate. Melting temperatures were determined from the second heating run.

2.3. Molar mass distributions

Wax S was dissolved in hexane to make a 0.5% solution. The samples were analysed and compared to a hydrocarbon standard using a Hewlett Packard 5890 Series II gas chromatograph with a split/splitless injector and a flame ionisation detector. The column was a 30 m × 0.25 mm i.d. Rtx-1 with 0.25 μm film thickness. The molar mass distribution of Wax FT was determined using high-temperature gel permeation chromatography. A flow rate of 1 mL min^{-1} on a PL-GPC 220 high-temperature chromatograph (Polymer Laboratories) was used and the measurement was performed at 160 °C. The columns used were packed with a polystyrene/divinylbenzene copolymer (PL gel MIIXED-B [9003-53-6]) from Polymer Laboratories. The sample concentration was 2 mg mL^{-1} and the solvent used was 1,2,4-trichlorobenzene, stabilized with 0.0125% 2,6-di-*tert*-butyl-4-methylphenol (BHT). BHT was used as a flow rate marker. The detector used was a differential refractive index detector.

2.4. Variable-temperature XRD measurements

Variable-temperature powder X-ray diffraction data were collected with Cu Kα radiation on a Panalytical X'Pert Pro MPD diffractometer. The sample stage used was an Anton Paar HTK1200N high-temperature chamber. Peak shifts due to variation in sample height were prevented by the use of a parallel X-ray beam from a primary beam PW3149/63 hybrid monochromator. Rapid data collection was achieved by using a fast X'Celerator RTMS detector. Tube settings: 40 kV and 40 mA. Step size: 0.0170° 2θ. Count time: 20 s per step.

3. Results and discussion

Over the past 8 years we have published a number of papers on polyethylene/wax blends [12–21]. All the waxes that we used showed multiple endothermic peaks in their DSC curves when analysed between ambient temperature and about 150 °C. For one of these waxes (called Wax S in this paper), the two peaks are well-resolved and we accepted, based on work summarized in Section 1 of this paper, that the first peak is the result of a solid–solid transition in the wax crystals, closely followed by a melting peak. In this paper we present and discuss results that confirm what we have assumed in our previous papers.

The second wax (Wax FT) was obtained from a different source, and forms part of a number of different waxes obtained through the Fischer–Tropsch process, which uses a standard starting material, syngas, rather than the more usual crude oil. This results in a more predictable and consistent end product free of sulphur, heavy metals and other polluting chemicals. Because of the way in which these products are formed, the specific properties of the products in terms of viscosity, melting point and so on can be tuned according to application needs. Since its DSC curve also shows multiple peaks, although more overlapped, it was important for us to establish whether one or more of these peaks may also be the result of solid–solid transitions in the wax crystals.

Fig. 1 shows the DSC heating curves for Wax S and Wax FT. Wax S shows two well-resolved endothermic peaks at 41 and 57 °C, respectively. Wax FT shows an endothermic peak maximum at 84 °C, followed by a peak shoulder at 91 °C, and a partially resolved peak at 105 °C.

The molar mass distribution curve for Wax S in Fig. 2 shows a single, well-defined and fairly narrow molar mass distribution ranging from about 320 to about 440 g mol^{-1}. This indicates an *n*-alkane mixture with chain lengths in the range C22–C30. Fig. 3 shows the XRD spectra of Wax S obtained every 5 °C from 30 to 60 °C. The XRD spectrum of the wax at room temperature shows two distinct peaks at 2θ = 21.2° and 23.5°. Between 35 and 40 °C, which is the temperature range where the DSC

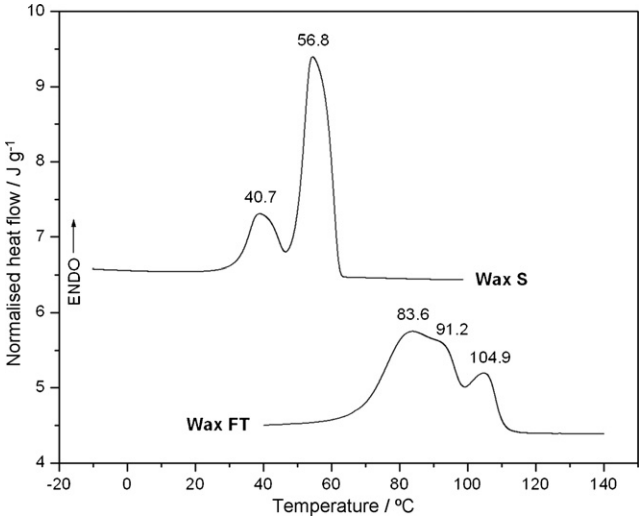

Fig. 1. DSC melting peaks of Wax S and Wax FT.

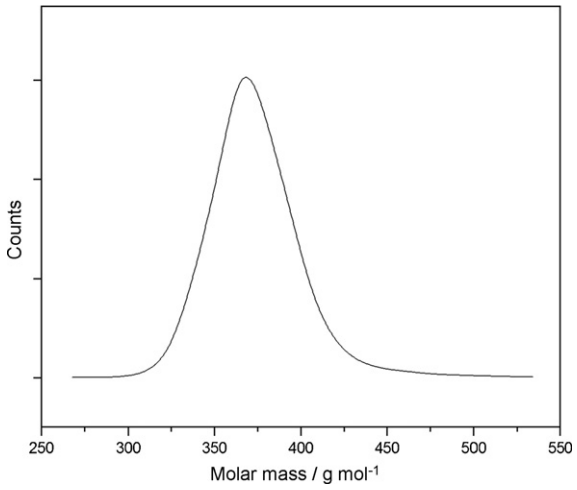

Fig. 2. Molar mass distribution curve for Wax S.

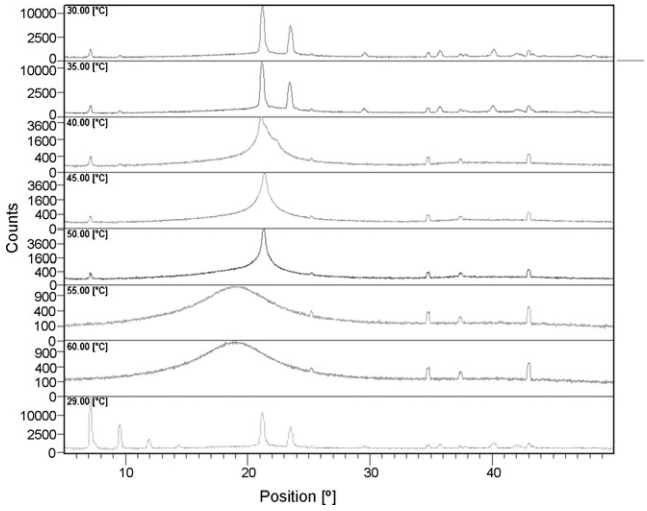

Fig. 3. Variable-temperature XRD spectra for Wax S.

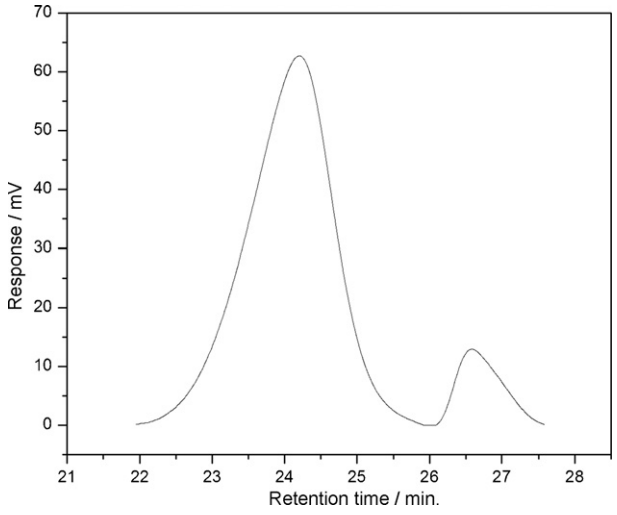

Fig. 4. Molar mass distribution curve for Wax FT.

heat flow first increases, there is a clear phase change which is completed at about 45 °C. This is the temperature at the minimum between the two DSC endotherms in Fig. 1. The first DSC peak is therefore clearly a solid–solid transition, probably an orthorhombic to hexagonal phase transition. On cooling the wax crystallizes with increased preference-orientation and the relative heights of the low-angle peaks ($2\theta = 7.2^\circ$, 9.5°, 12.0°) increase, but the pattern is still the same.

Contrary to the Wax S case, the molar mass distribution curve for Wax FT shows two well-resolved peaks with peak maxima at retention times of, respectively, 24 and 26.5 min, indicating distinctly different molar mass fractions (Fig. 4). Different melting behaviour of these molar mass fractions is probably the reason for the multiple melting peaks observed in Fig. 1. Heating of this wax after fractional crystallization using DSC (Fig. 5 [22]) shows very little difference in the multiple peak arrangement. The first peak moved to a slightly lower temperature, while two peaks seem to have developed at temperatures slightly lower and slightly higher than the peak temperature of the last peak in the DSC curve of Wax FT in Fig. 1. This confirms that distinctly

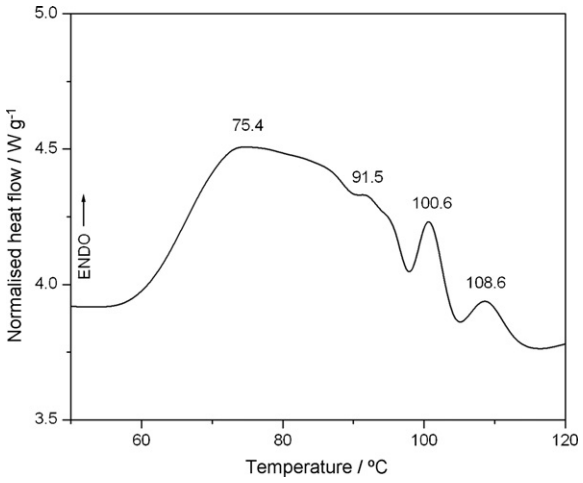

Fig. 5. DSC melting peaks, after thermal fractionation, of Wax FT.

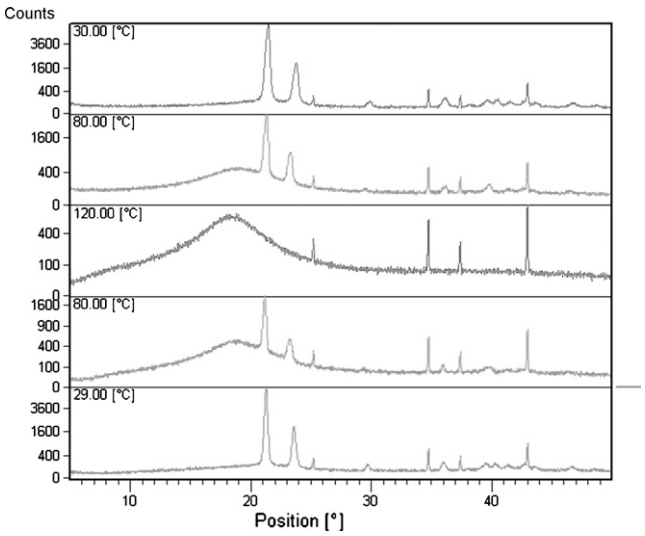

Fig. 6. Variable-temperature XRD spectra for Wax FT.

different thermal fractions have already existed in the neat wax. The XRD spectra of Wax FT at different temperatures in Fig. 6 show two distinct peaks at $2\theta = 21.2^\circ$ and 23.5° at room temperature. The shapes and positions of these peaks remain unchanged throughout the heating cycle. The amorphous diffraction halo of the wax melt is already visible at 80 °C, which is below the peak temperature of the first peak in the DSC heating curve. At 120 °C, which is immediately after the last peak of the multiple peaks in the DSC heating curve, the amorphous halo has completely replaced the diffraction peaks. On cooling the amorphous halo disappears and the diffraction peaks appear without any change in crystal structure.

4. Conclusions

Two waxes, a soft petroleum wax and a hard Fischer–Tropsch paraffin wax, have been investigated to confirm the reasons for the multiple endothermic peaks observed during the heating of these waxes in a differential scanning calorimeter (DSC). DSC curves before and after thermal fractionation, molar mass distribution curves, and variable-temperature XRD results were compared, and it was confirmed that the first endothermic peak for the soft petroleum wax was due to a solid–solid transition, while the second endothermic peak was due to melting. However, for the hard Fischer–Tropsch paraffin wax there was no evidence of a solid–solid transition, and it was concluded that the multiple endothermic peaks in this case were due to melting of different molar mass fractions.

Acknowledgements

Prof. Gert Kruger from the Department of Chemistry, University of Johannesburg, South Africa did the variable-temperature XRD analyses. The GC analysis was done at the Council for Scientific and Industrial Research in Pretoria, South Africa, and the GPC analysis was done at the Polymer Institute, University of Stellenbosch, South Africa. The National Research Foundation (GUN 2070099) and the University of the Free State in South Africa are acknowledged for financial support.

References

[1] F. Asinger, Paraffins: Chemistry and Technology, Pergamon Press, 1967.
[2] H. Inaba, P. Tu, Heat Mass Transfer 32 (1997) 307.
[3] A. Sari, Energy Convers. Manage. 45 (2004) 2033.
[4] B. Zalba, J.M. Marin, L.F. Cabeza, H. Mehling, Appl. Therm. Eng. 23 (2003) 251.
[5] A.M. Khudhair, M.M. Farid, Energy Convers. Manage. 45 (2004) 263.
[6] S.M. Hasnain, Energy Convers. Manage. 39 (1998) 1127.
[7] Z. Zhang, X. Fang, Energy Convers. Manage. 47 (2006) 303.
[8] A. Hammami, A.K. Mehrotra, Fuel 74 (1995) 96.
[9] G. Ungar, N. Masic, J. Phys. Chem. 89 (1985) 1036.
[10] S.J. Severtson, M.J. Nowak, Langmuir 18 (2002) 9371.
[11] A. Genovese, G. Amarasinghe, M. Glewis, D. Mainwaring, R.A. Shanks, Thermochim. Acta 443 (2006) 235.
[12] I. Krupa, A.S. Luyt, Polym. Degrad. Stabil. 70 (2000) 111.
[13] I. Krupa, A.S. Luyt, Polymer 42 (2001) 47.
[14] I. Krupa, A.S. Luyt, Polym. Degrad. Stabil. 73 (2001) 157.
[15] I. Krupa, G. Miková, A.S. Luyt, Eur. Polym. J. 43 (2007) 895.
[16] I. Krupa, G. Miková, A.S. Luyt, Phase change materials based on low-density polyethylene/paraffin wax blends, Eur. Polym. J. 43 (2007) 4695.
[17] I. Krupa, A.S. Luyt, J. Appl. Polym. Sci. 81 (2001) 973.
[18] T.N. Mtshali, A.S. Luyt, I. Krupa, Thermochim. Acta 380 (2001) 47.
[19] S.P. Hlangothi, I. Krupa, V. Djokovic, A.S. Luyt, Polym. Degrad. Stabil. 79 (2003) 53.
[20] I. Novak, I. Krupa, A.S. Luyt, J. Appl. Polym. Sci. 95 (2005) 1164.
[21] M.J. Hato, A.S. Luyt, J. Appl. Polym. Sci. 104 (2007) 2225.
[22] V. Chevallier, E. Provost, J.B. Bourdet, D. Petitjean, M. Bouroukba, M. Dirand, Polymer 40 (1999) 2121.
[23] V. Chevallier, D. Petitjean, M. Bouroukba, M. Dirand, Polymer 40 (1999) 2129.
[24] M. Zheng, W. Du, Vib. Spectrosc. 40 (2006) 219.
[25] T. Górecki, S.P. Srivastava, G.B. Tiwari, Cz. Górecki, A. Żurawska, Thermochim. Acta 345 (2000) 25.
[26] E.B. Sirota, A.B. Herhold, Polymer 41 (2000) 8781.